MDPI

Article

Remanufacturing the AA5052 GTAW Welds Using Friction Stir Processing

Ghasem Azimi Roeen [1],*, Sajjad Ghatei Yousefi [2], Rahmatollah Emadi [2], Mohsen Shooshtari [3] and Saeid Lotfian [4],*

[1] Center of Educational Workshops, Isfahan University of Technology, Isfahan 8415683111, Iran
[2] Department of Materials Engineering, Isfahan University of Technology, Isfahan 8415683111, Iran; ghatesajjad144@gmail.com (S.G.Y.); remadi@iut.ac.ir (R.E.)
[3] Department of Biosystem Engineering, Isfahan University of Technology, Isfahan 8415683111, Iran; mohsen_shooshtari@yahoo.com
[4] Naval Architecture, Ocean and Marine Engineering Department, University of Strathclyde, Glasgow G1 1XQ, UK
* Correspondence: azimi_gh@iut.ac.ir (G.A.R.); saeid.lotfian@strath.ac.uk (S.L.); Tel.: +44-(0)-141-5484371 (S.L.)

Abstract: Progress in sustainable manufacturing is a crucial element to minimise negative environmental impacts. The conventional fusion weld process used to join aluminium alloys resulted in coarse grain structure, inevitable defects, and severe joint softening. Friction stir processing (FSP) has the potential to modify the microstructure of materials in joint structure and improve the mechanical properties. In this investigation, the effect of friction stir post–processing was evaluated to study the microstructural characteristics and mechanical properties of GTAW (gas tungsten arc welding) welds in the aluminium 5052 alloy. During FSP, the grains' dendritic microstructure was destroyed, and the dynamic recrystallisation resulted in a very fine and equiaxed grains structure in the fusion zone. The hardness of the friction-stir-processed welds significantly improved because of microstructure grain refinement. The processed joint demonstrated higher ultimate tensile and yield strength (~275 MPa and 221 MPa, respectively) and superior elongation (31.1%) compared to the unprocessed weld; at the same time, the mechanical strength (yield and ultimate tensile) is similar to that of the base metal.

Keywords: remanufacturing; grain reinement; friction stir processing; GTAW; 5052 aluminium alloy; AA5052

1. Introduction

The traditional model is defined based on the "take-make-consume-waste" approach, and it consumes resources. Transferring from the linear model and moving to a generative and restorative model based on the circular economy concept is crucial. The main target in the circular economy model is to keep products and components at their highest efficiency and value, alongside their maximum lifecycle. [1,2]. Remanufacturing and proactive maintenance are considered the best recovery strategies for environmental benefit and economic viability [3,4]. Among various joining processes, welding is commonly used in the manufacturing industry due to its evident advantages. Welding plays a significant role when it comes to the fabrication of large and complex components and structures [5–7].

Aluminium alloys are generally utilised in structural applications such as aerospace, automobile industries, railway vehicles, bridges, offshore structure topsides, and high-speed ships, due to their light weight and higher strength-to-weight ratio. Welding is categorised as the foremost joining strategy, but it has always been associated with many technological challenges. Some difficulties are associated with the aluminium welding joint process, mostly related to a rigid and hard oxide layer, high thermal conductivity, high coefficient of thermal expansion, shrinkage during solidification, and molten state hydrogen solubility [7–10]. AA5052 has exceptional corrosion resistance against seawater and salt

spray, making it the primary candidate for marine application, particularly for failure-sensitive large structures [11]. GTAW and gas metal arc welding (GMAW) are the preferred welding processes for the 5xxx alloys, as they are relatively easy to apply and cost effective. Despite much progress in technologies and welding materials, welding of 5xxx alloys still remains a challenge [7,9]. Besides common defects, such as distortion and porosity, serious problems could arise for weld joints due to hot cracking in the weld and softening in the weld fusion zone and heat-affected zone (HAZ). The predominant thermal conditions during the solidification of weldment lead to a coarse columnar grains microstructure in the fusion zone. Such a microstructure tends to demolish mechanical properties and increase susceptibility to solidification cracking. Therefore, it is crucial to control the solidification microstructure. It is noteworthy, because of the high temperature and thermal gradient, that such control is often unmanageable. Nonetheless, a few techniques, such as using pulsed current welding, the arc manipulation technique, and torch vibration for refining the microstructure of fusion zones, have been investigated. Despite the promising laboratory results, using such a method may increase the complications during manufacturing [12–19].

The weldments need to go through remanufacturing procedures to overcome the difficulties caused by coarse-grain structures. The remanufacturing processes could include post-welding treatment such as hammering and shot peening. Applying these types of methods improves the mechanical properties of the weldment. It changes the surface residual tensile stress of the fusion weld to residual compressive stress, which is beneficial and enhances the weld performance, durability, and reliability [16,17]. Using friction stir welding (FSW), a solid-state process, has the advantage of preventing the issues related to solidification in conventional welding technologies [20]. Friction stir processing (FSP) is a development from FSW, and it can be used for structural refinement to enhance the material property. In FSP, a rotating non-consumable tool generates stirring and mixing in solid-state; therefore, materials experience severe plastic deformation. The complex thermomechanical processes inside the stir zone result in significant microstructural modifications. FSP can be used as a remanufacturing process, and can follow fusion welding processes such as GTAW. It is expected that applying FSP can modify weldment in addition to microstructural refinement. The approach can potentially eliminate defects and mechanical properties in the weld joint [6,20–23]. Silva et al. and Costa et al. achieved superior mechanical properties in 6082-T651 alloy GMAW butt and T-fillet welds with FSP [24,25]. Mandal successfully used multipass FSP for surface modification of 7xxx series aluminium alloy [26]. Mehdi et al. investigated the effect of post-FSP on GTAW dissimilar welded joint of AA6061 and AA7075. Based on their results, FSP significantly amended the mechanical properties of the weld joint [27]. Most of the studies were carried out on heat-treatable aluminium alloys such as the 2xxx, 6xxx, and 7xxx series. In addition to the effect of alloying elements, the strengthening mechanisms in these alloys are precipitation hardening. These heat-treatable alloys were subjected to partial annealing during the welding operation. The final FSP decreased the grain sizes, eliminated the welding defects, and homogenised the distribution of solid solution in the stir zone to be ready for the post-process heat treatment [20,28].

In non-heat-treatable aluminium alloys such as the 5xxx series, alongside the effect of alloying elements, the main mechanism for strengthening is strain hardening. The non-heat-treatable alloys are annealed in the heat-affected zone adjacent to the weld, which is unavoidable during conventional fusing welding. A few studies are reported on the impact of post-FSP on the welded joint. Fuller et al.'s investigation exhibited that FSP can be used to considerably enhance the monotonic tensile strength, yield strength, and elongation of AA5083-H321 arc welds [14]. During the last decade, aluminium alloys of the 5xxx series were commonly used as structural materials in offshore energy applications due to their high corrosion resistance in a harsh environment. There are a few studies considering the maintenance/remanufacturing of these structural materials in marine energy sectors. Enhancing the corrosion resistance and increasing the structural fatigue life is possible by controlling the kinetics of the dominant corrosion types, which need to govern the residual stresses in the weldment. Post-FSP could enhance the mechanical strength of the weldment

by overcoming the annealing effect after the conventional fusing welding process. In the present research, the FSP was carried out as a post-process on the AA5052 GTAW butt weld joint. Besides, the effect of the FSP was investigated on the microstructural evolution and materials characteristics.

2. Materials and Methods

Two-millimetre-thick aluminium AA5052 alloy was used in this research as the base metal. The sheet was sliced to get ready workpieces with a length and width of 150 mm and 30 mm, respectively (Figure 1a). Base material samples were GTAW welded on, utilising an industrial ER5356 filler wire with a diameter of 2.4 mm. The chemical compositions and mechanical properties of base and filler metals are shown in Table 1. Before being welded, the plates were oxidised with a dilution of 40 grams sodium hydroxide and 1 litre water for 50 s. The plates' edge was brushed with a steel wire brush to remove the oxide layer just before welding. Samples were cleaned with acetone to omit welded metal porosity and to remove oil and dirt.
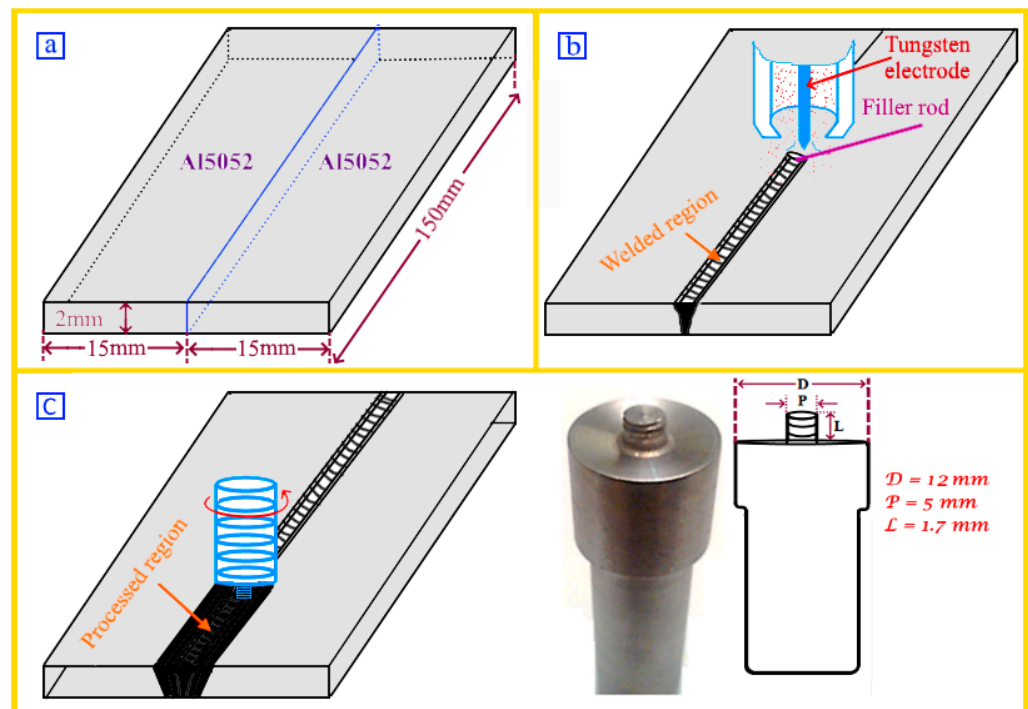
Figure 1. Schematics that show (**a**) sample size, (**b**) GTAW process, and (**c**) friction stir process.

Table 1. Chemical compositions and mechanical properties of base metal (AA5052) and filler metal (ER5356).

Material	Zn	Fe	Cr	Mn	Ti	Cu	Si	Mg	Al
Base metal	0.004	0.096	0.295	0.2	0.045	-	0.172	2.744	rest
Filler metal	0.1	0.4	0.05–0.2	0.05–0.2	0.06–0.2	0.1	0.25	4.5–5.5	rest

Mechanical Properties	Yield stress (MPa)		Tensile stress (MPa)		Elongation(%)	
Base metal	210		254		16	
Filler metal	120		240		17	

While welding was being processed in the inert media, argon shielding gas was used to protect the weld pool from the dissolution of atmospheric gases. For GTAW welding, an automatic KEMPPI Kempotig AC/DC 250, (Kemppi GmbH, Langgöns, Germany) commercially available machine was used in the way of one-passed welding (Figure 1b).

Several experiments were held to obtain the optimum parameters in GTAW processing. As a result, the best characters of joints were found out, as shown in Table 2.

Table 2. Optimum parameters for GTAW of AA5052.

Filler Material	Welding Current (A)	Speed (mm/min)	Gas Flow Rate (L/min)	Torch Angle
ER5356	68	100	8	45–60

After that, friction stir post-processing was done on the GTAW welds' top surfaces to 1.7 mm deep (Figure 1c). A fixture was designed and fabricated in the workshop considering the welding specimens' size. The weldments were fixed on the workbench using the designed fixture with several toggle clamps. FSP was carried out through a straight cylindrical tool (pin diameter and length: 5 mm and 1.7 mm, respectively; shoulder diameter: 12 mm) made of heat-treated high carbon steel (H13). In addition, grooves with 0.5 mm pitch length had been cut into the pin to have a better mixture in the weld pool. The FSP parameters were tool rotation speed of 800 rpm, travelling speed of 60 mm/min, and tool tilt at 3° backward from the vertical.

To study the microstructural evolution, samples were cut off in weldment cross-sections transversely; thus, the specimens included the FSP and unprocessed areas. The standard metallographic coupons were prepared from the cut specimens. For etching, the polished surfaces Tucker's reagent (80 mL H_2O, 40 mL HNO_3, 2.5 mL HF, 30 mL HCl, 12 g CrO_3, and 0.25 of a drop H_2O_2) was used.

Microstructural details were provided using optical (OM, Olympus GX51, Olympus Ltd., Tokyo, Japan) and scanning electron microscopes (SEM, FEI Philips XL 30, Philips, The Netherlands). The SEM was equipped with electron back-scattered diffraction (EBSD; X-Max, Oxford Instruments, Abingdon, UK) detectors. X-ray diffraction (X-Pert, XRD, PMD Philips, São Carlos, Brazil) is used to recognise the stir zone (SZ) phases. Moreover, to evaluate the mechanical properties of weldments, the Buehler Micromet Microhardness Tester (Buehler Ltd., Lake Bluff, IL, USA) and Hounsfield universal tensile testing machine (Model H25KS, UK) were used. The microhardness was measured along the transverse cross-section of the welded specimen using a load of 0.05 kgf and a stay time of 10 s with 500 µm between each point. The tensile test of the welded samples was conducted following the ASTM E8M-04 standard [29], and at least three specimens were used for all mechanical tests. All the experimental coupons were tested at room temperature, applying a low speed of 1 mm/min. Each joint was measured with at least three tensile and hardness samples chosen from the same joint to reach reliable strength and hardness measurements.

3. Results and Discussion

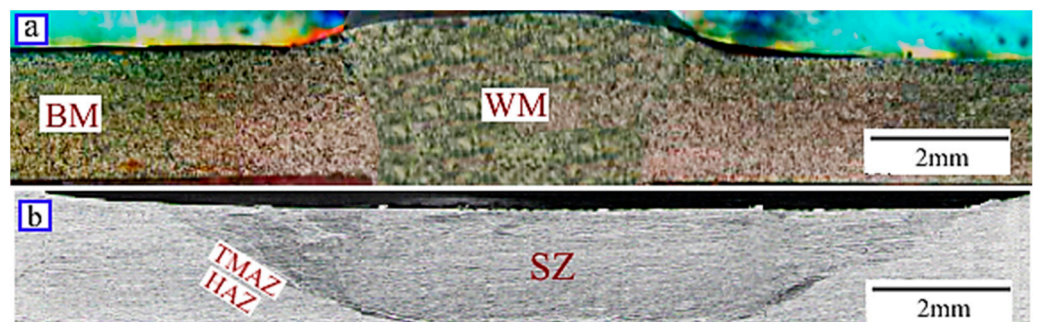### 3.1. Microstructures

The microstructure images of the base metal in the rolling direction and perpendicular to the rolling direction are shown in Figure 2. As can be seen, grains are elongated in the rolling direction (Figure 2a). The base metal's microstructure perpendicular to the rolling direction was formed with rather coarse and equiaxial grains (Figure 2b). The "Image J" software (1.45f version—National Institutes of Health, Bethesda, MD, USA) was used to analyse the grain size perpendicular to the rolling direction, and it showed that the mean grain size was 30–40 µm.

Low-magnified cross-sectional images of the unprocessed and friction-stir-processed weldment are shown in Figure 3. As illustrated in Figure 3a, GTAW weld has complete penetration without a lack of fusion and porosity. As can be seen in the cross-section of the FSP specimen (Figure 3b), the sample has no defects, such as tunnel defect and reduction of thickness in the stir zone (SZ), compared with the base metal.
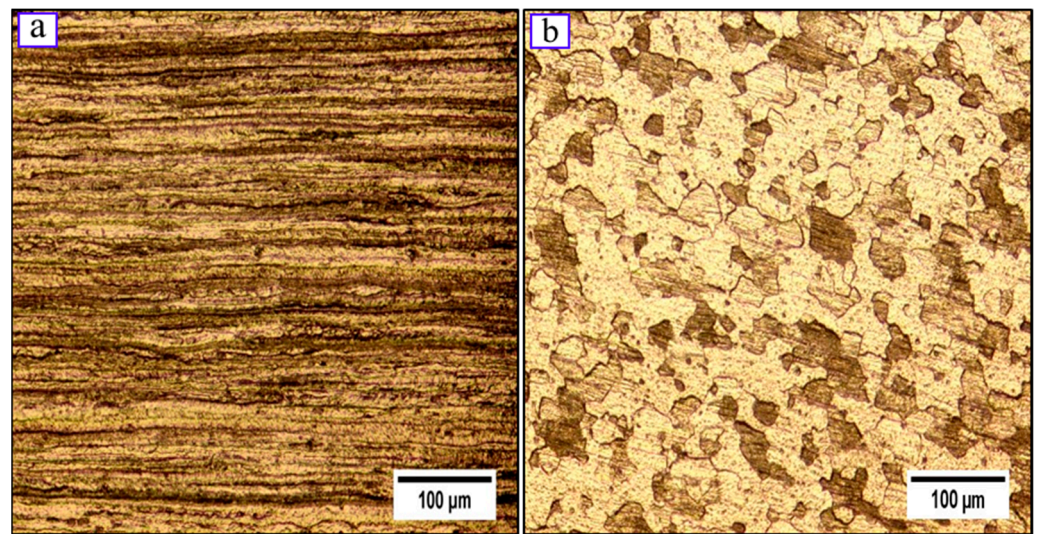
Figure 2. Microstructure image of the base metal: (**a**) in the rolling direction, (**b**) perpendicular to the rolling direction.

Figure 3. Optical micrographs showing the cross-section of the (**a**) unprocessed and (**b**) friction-stir-processed weldment.

Figure 4 shows the microstructure of the weld of both samples (unprocessed and processed with FSP) in a weld cross-section at higher magnification. Various zones are visible, as indicated in the images. The microstructure of the base metal is entirely altered after the welding process. The grains are coarser and equiaxial, which can be seen in the HAZ and partially melted zone (PMZ). Those coarser grains were formed at high temperatures close to the melting zone (Figure 4a).
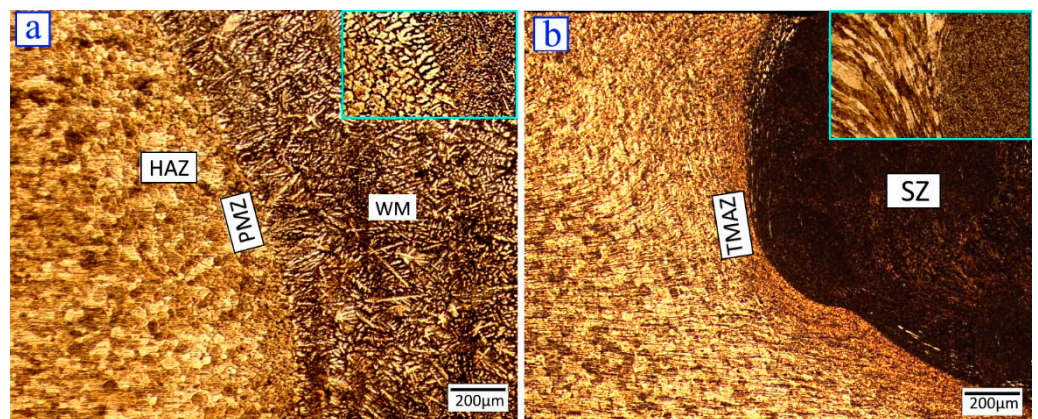
Figure 4. Optical micrographs of the weld: (**a**) unprocessed and (**b**) processed with FSP.

PMZ is the narrow region between weld metal and base metal, located immediately outside the fusion zone. In the fusion line, grains of base metal act as local nucleation sites, and because the liquid material in the weld melt pool is in direct contact with these grains, the recrystallisation process take control. It means new grains recrystallise on these grains, and the growth happens in the easy orientation (e.g. <100> in the FCC structures), resulting in the epitaxial growth in PMZ that is shown in Figure 4a. Solidification happens spontaneously by epitaxial growth on the partially melted grains. Thus, the fusion zone (FZ) grains structure is principally controlled by the base metal microstructure and welding parameters and conditions [30].

Cross-sectional images of the FSP sample (Figure 4b) show separate zones, including stir zone (SZ), thermo-mechanically affected zone (TAMZ), heat-affected zone (HAZ), and base metal (BM). As depicted in Figures 3b and 4b, using a proper rotational and transitional speed in FSP led to sufficient heat input and convectional flow material, which results in a homogenous structure without any common defects such as tunnel and porosity. Moreover, TMAZ and SZ zones are completely clear in Figure 4b. SZ is composed of fine-equiaxed recrystallised grains. The fine recrystallised grains at the SZ are formed due to severe plastic deformation, followed by dynamic recrystallisation resulting from the thermo-mechanical processing [12,15,31,32].

TMAZ, which is close to the SZ, exhibits almost the same microstructure, both at the retreating side (RS) and advancing side (AS), but the RS's microstructure seems to be a little elongated because of more local heat (Figure 5). TMAZ exhibits elongated grains compared to the AS and RS due to stirring; however, it is worth noting that the microstructure in this zone is not recrystallised. In addition, the heat generated during the welding transmitted away from the welding zone through the metal body. It formed the HAZ region, which is between the melted metal and the unaffected base metal. It is noteworthy that HAZ and PMZ of fusion welding are placed in TMAZ, and because of the high plastic strain in these zones, grains were elongated and oriented. During the FSP, due to the lower temperature in the processed sample, the HAZ region was smaller and contained a finer grain size (Figure 6).
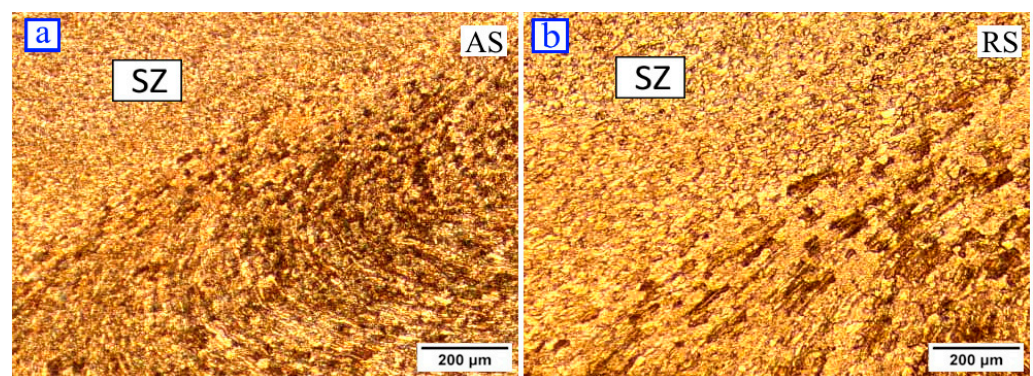

Figure 5. Optical micrographs of the weld after FSP: (**a**) advancing side and (**b**) retreating side.

Figure 7 shows the microstructure of the base alloy (Figure 7a), unprocessed (Figure 7b), and friction-stir-processed (Figure 7c) welds. In the weld zone, the high welding temperature caused a higher cooling rate throughout solidification and increased nucleation sites. Compared to the growth rate, the higher nucleation rate causes a more refined grain structure with various equiaxed dendritic sizes (Figure 7b). During FSP, the rotating pin generates stirring and mixing in welding and HAZ regions; therefore, materials experience severe plastic deformation in the processed zone. As a result, fine equiaxed recrystallised grains are formed [6,21,28,33]. Thus, as shown in Figure 7c, the dendrite structure resulting from fusion welding is totally destroyed. Due to dynamic recrystallisation, a very fine and equiaxed grains microstructure has been created. The grain boundaries image after FSP is

shown in Figure 8a. The mean grain size of the friction-stir-processed weld was measured to be ~3 μm.
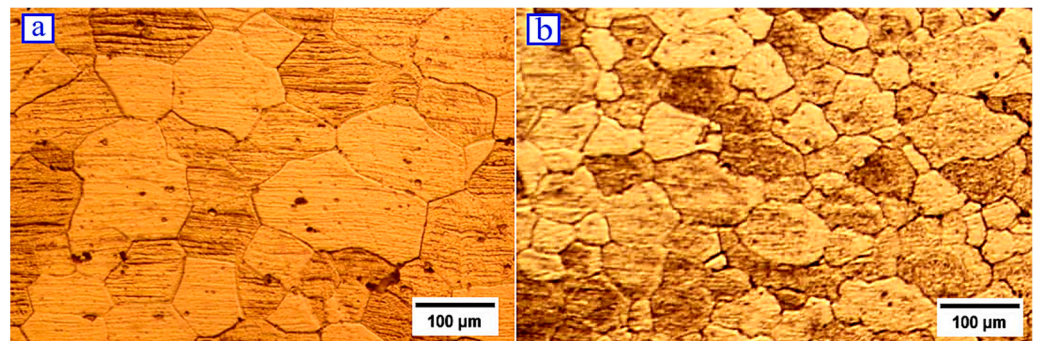
Figure 6. Optical micrographs of HAZ: (**a**) unprocessed and (**b**) processed with FSP.
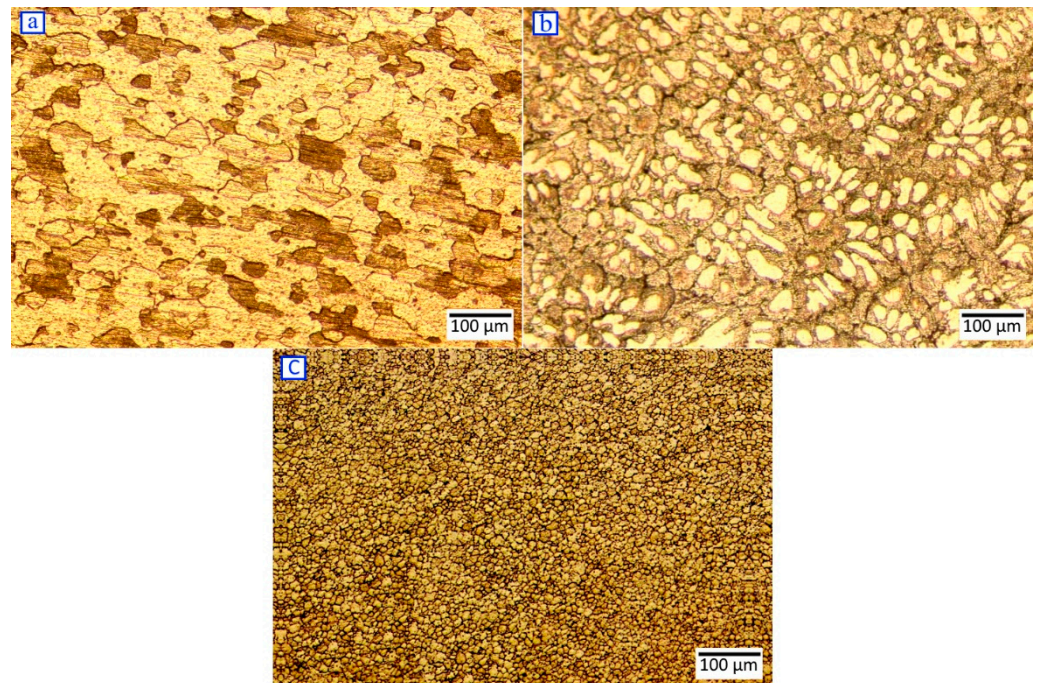

Figure 7. The microstructure of (**a**) the base alloy, (**b**) unprocessed, and (**c**) friction-stir-processed welds.

FSP is a hot working process. The dynamic recovery, recrystallisation, and grain growth phenomenon happen simultaneously due to intensive plastic deformation in high relative temperature. Furthermore, in the metals with high stacking fault energy, such as aluminium, movement and slip of dislocations happen easier during hot working, and as a result, the dynamic recovery occurs readily [33,34].

Moreover, as mentioned, FSP is a high-temperature, severe-plastic-deformation process that eventuates in very fine grains formation in the stirred zone due to dynamic recrystallisation. Continuous dynamic recrystallisation (CDRX) contains two stages, which are the formation of low-angle grain boundaries (LAGBs) and conversion from LAGBs to high-angle grain boundaries (HAGBs). The FSP specimen exhibited a high fraction of fine grains and confirmed the average grain size of ~3 ± 0.5 μm, with large HAGB fractions of ~52% (Figure 8b). The dark lines in this orientation map represent HAGBs (>15° misorientation). In the first stage, LAGBs are formed during hot working by the recrystallisation mechanism being dominant. The misorientation at LAGBs rises steadily until the transient to HAGBs happens. The LAGBs transforming rate depends on the pinning of subgrain

boundaries [31,33–35]. After an apparent deformation level, the sub-boundaries are pinned by precipitates in the matrix (or effect of some solid solution elements). These boundaries will act as a continuous trap for dislocations. X-ray diffraction (XRD) patterns of base metal, unprocessed, and friction-stir-processed welds are depicted in Figure 9. According to the figure, the intensity of peaks for the FSP weld is diminished compared to the base and unprocessed weld, and added to its width. This is related to the increasing and decreasing lattice strain and crystallite size, respectively.
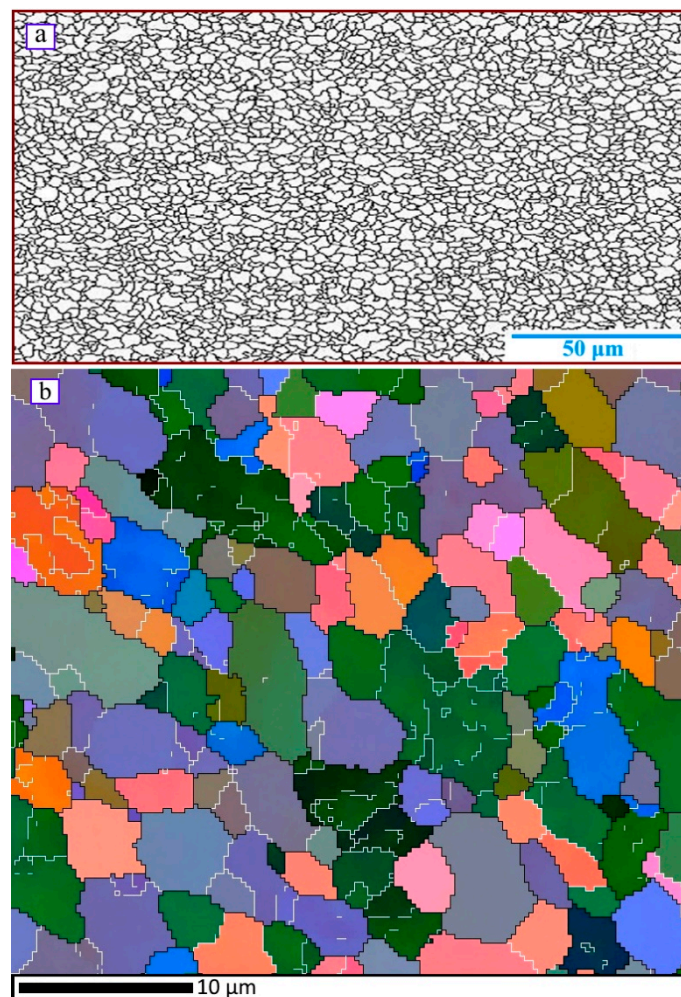
Figure 8. (**a**) Optical micrograph of grain boundaries image of FSP specimen, (**b**) EBSD orientation map (white colour for LAGBs and black colour for HAGBs).

3.2. Mechanical Properties

The aluminium alloy used in this investigation was in rolling condition. Appraising the welding process on this alloy shows significant changes in mechanical properties of weldment metal regions and HAZ. Figure 10 shows the micro-hardness profiles related to central cross-sectional zones of the unprocessed and friction-stir-processed welds. It should be noted that the average hardness of the base metal was 60 HV. Regarding the hardness curve of GTAW weldment, weld metal and HAZ illustrate maximum and minimum hardness, respectively. This could be explained by the noticed fine-grain structures and the existence of magnesium. In fact, the hardness increases due to the fine co-axial dendritic structure, intermetallic compounds, the precipitates forming, and the high cooling rate in the weld metal region [7,13]. As a result of the interaction between the grain growth and precipitates' existence in the HAZ, hardness has moderately reduced.
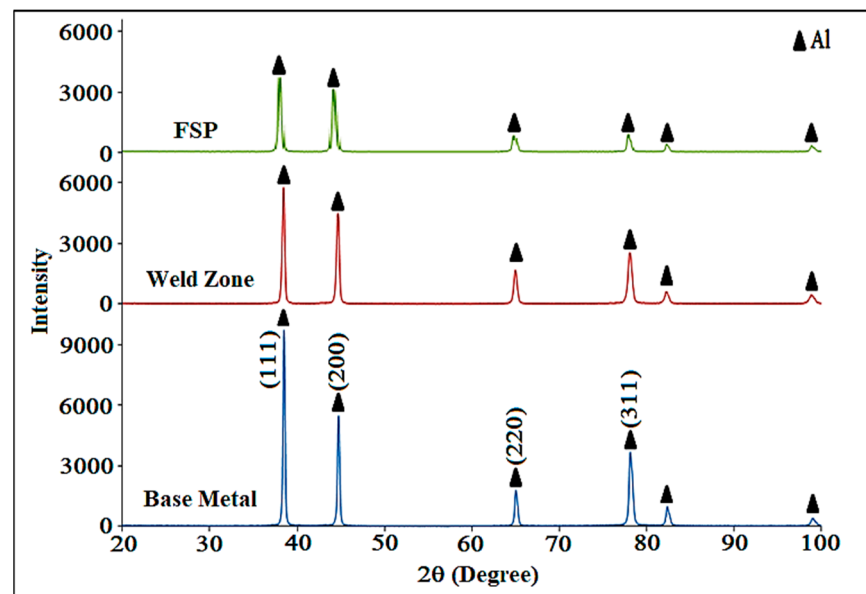
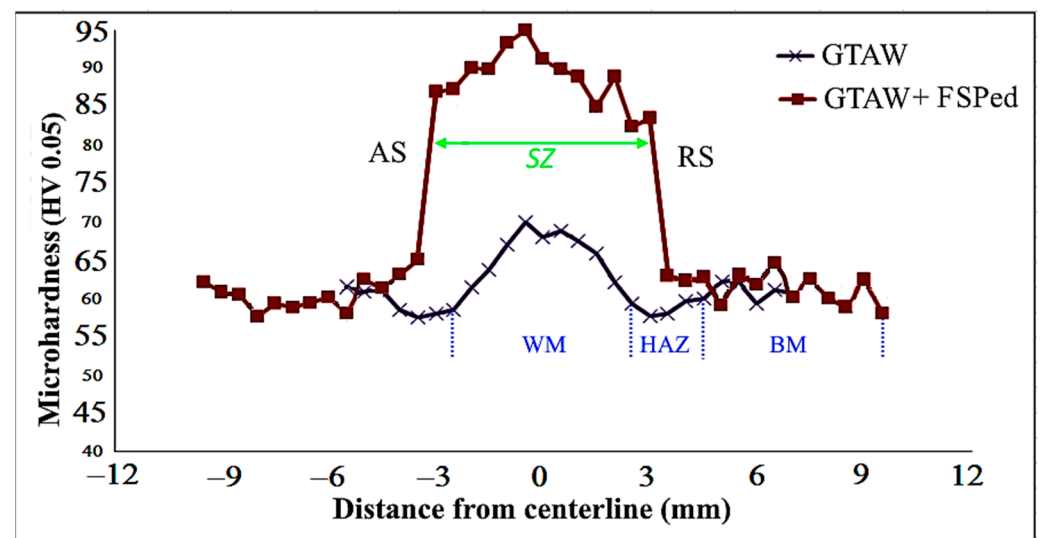**Figure 9.** X-ray diffraction pattern of base metal, unprocessed, and friction-stir-processed welds.

Figure 10. Microhardness profiles of the central cross-sectional zones of the unprocessed and friction-stir-processed welds.

FSP causes the elimination of weldment structure by crushing and uniform distribution of precipitates, as well as forming refined co-axial grains thanks to the dynamic recrystallisation phenomenon. Hardness has an inverse relation with grain size based on the Hall-Petch equation [36]. Therefore, it is expected that hardness increases in the central region of the SZ. As shown in Figure 10, the use of FSP on the GTAW weld induced a significant increase of the hardness values. The rise in hardness is because of the recrystallised grains, low entrance heat, faster cooling per unit length of the weld, and uniform distribution of intermetallic precipitates [14]. Furthermore, coarse grains in HAZ are deformed due to the severe plastic deformation induced by the tool shoulder. Hardness also increases in this area. Notably, hardness in the AS is slightly higher than the RS. In the AS, the rotational tool's linear velocity and total displacement vector of the rotational tool are in the same direction on the aluminium alloy surface. Consequently, the sum of these two vectors results in higher linear motion in this area. However, on the retreating side, the direction of the mentioned vectors is the opposite, and thus the sum of them attains a lower linear velocity. This difference in linear velocity value of mentioned zones

leads to microstructure differences of the two areas and, finally, different hardnesses in these regions.

The tensile test results for the BM, unprocessed, and friction-stir-processed welds are shown in Figure 11. As can be seen, for unprocessed weld, yield and ultimate tensile strength are lower than BM, while elongation is higher. As a result of fusion welding, BM's rolled structure with high dislocations density is changed to the dendrite structure with equiaxed and fine grains that increase the elongation. It is noteworthy that the fracture in this specimen occurred in the HAZ. This region has the lowest hardness because of grain growth. As illustrated in Figure 11, the processed weld showed better performance during the tensile test. FSP was found to improve mechanical properties, with the ultimate tensile strength and elongation increasing to 275 MPa and 31.1%, respectively. The results show that the maximum tensile strength of the friction-stir-processed weld is 11% higher than the unprocessed weld's tensile strength. In general, this increase can be attributed to the dissolution of some precipitates in the grain boundaries during recrystallisation (migrating grain boundaries dissolve small precipitates), uniform distribution of precipitates, strain hardening, and refinement of grains. It is worth noting that the refinement of grains is an effective manner to improve mechanical properties. By comparison between the strength results in base materials and FSP samples, it can be concluded that FSP effectively acts as a remanufacturing process, and mechanical properties of the FSP-welded joint are recycled. The yield and tensile strengths in FSP specimens are close to the individual base material before joining.
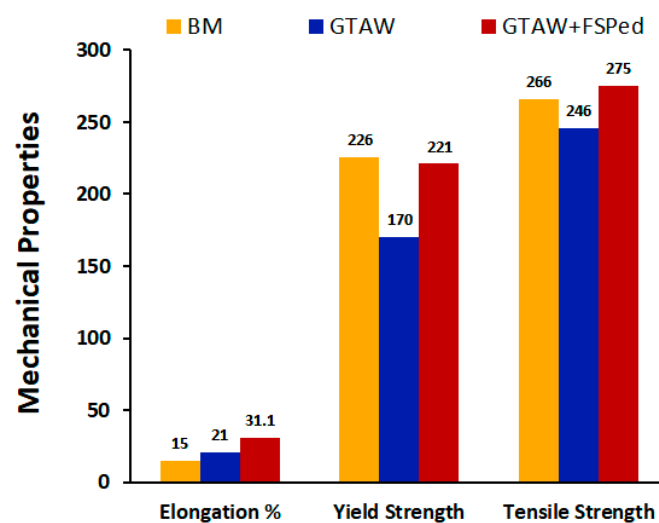
Figure 11. The yield strength, ultimate tensile strength (UTS), and elongation of the base material, unprocessed weldment, and friction-stir-processed welds.

Figure 12 shows the tensile fractured micrograph's SEM images related to as-received Al, unprocessed, and friction-stir-processed welds. Comparison between rolled (as-received) Al and unprocessed weld shows the dimensions and sizes of dimples are slightly smaller and more uniform in unprocessed weldment fractography. The SEM fractography shows a minor fraction of brittle fracture in this sample, which can be due to more dissolution and crushing of precipitates in the grain boundaries and the increase of sub-boundaries because of grains refinement. The processed specimen demonstrates a ductile fracture mode. The fracture surface of this specimen consists of fine dimples, which indicate the ductile fracture mechanism. As stated earlier, the dissolution of some precipitates, uniform distribution of precipitates, and refinement of grains transfer the fracture mode from a combined ductile-brittle rupture to a fully ductile fracture. Since the grain boundaries are the nucleation sites for micro-cracks during the fracture, the dimples' size is directly related to the grain structure.
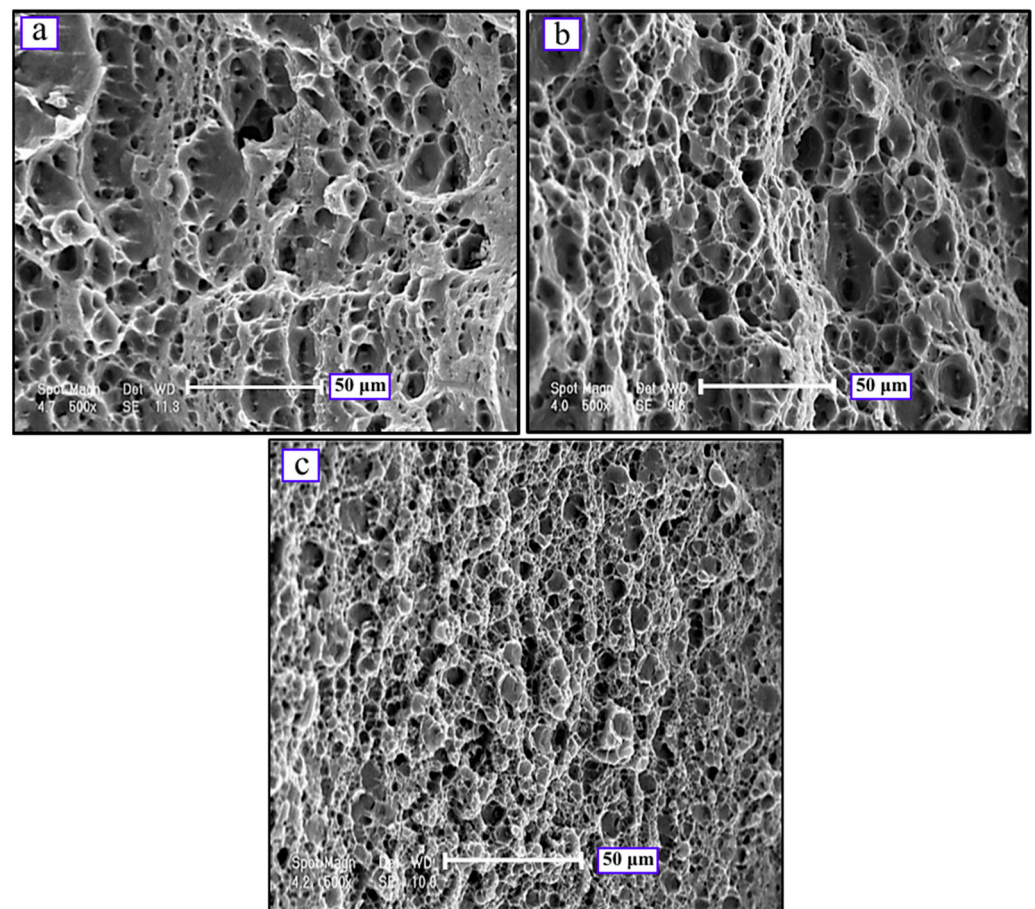
Figure 12. SEM images related to the tensile fractures of (**a**) as-received Al alloy, (**b**) unprocessed weld, and (**c**) friction-stir-processed weld.

4. Conclusions

In this study, the effect of friction stir post-processing on AA5052 aluminium GTAW welds has been investigated. The crucial findings are outlined as follows:

- Friction stir post-processing can be used as a remanufacturing technique to improve the AA5052 weldment and eliminate the issues caused by the GTAW welding process.
- Microstructural examination revealed the friction stir post-processing's influential role in generating fine equiaxed grains in the fusion zone. The significant grain refinement after FSP exhibited the occurrence of dynamic recrystallisation in the weld metal.
- The hardness of the friction-stir-processed welds was improved compared to the base metal and GTAW welds.
- Friction stir post-processing improves UTS and elongation of the weld joint. It is found that the friction-stir-processed weld presented 11% higher UTS and 32% higher elongation as compared to the unprocessed one. The processed specimen demonstrated a ductile fracture mode.

Author Contributions: Conceptualisation, G.A.R., R.E. and S.L.; methodology, G.A.R., R.E., S.G.Y. and S.L.; investigation, G.A.R., R.E., S.G. and M.S.; writing—original draft preparation, G.A.R. and S.L.; writing—review and editing, G.A.R., R.E. and S.L.; supervision, S.L., G.A.R., and R.E.; data curation, G.A.R. and S.L. All authors have read and agreed to the published version of the manuscript.

Data Availability Statement: The data presented in this study are available on request from the corresponding author. The data are not publicly available because it also forms part of an ongoing study.

References

1. Kerin, M.; Pham, D.T. Smart remanufacturing: A review and research framework. *J. Manuf. Technol. Manag.* **2020**, *31*, 1205–1235. [CrossRef]
2. Singhal, D.; Tripathy, S.; Jena, S.K. Remanufacturing for the circular economy: Study and evaluation of critical factors. *Resour. Conserv. Recycl.* **2020**, *156*, 104681. [CrossRef]
3. Lee, C.-M.; Woo, W.-S.; Roh, Y.-H. Remanufacturing: Trends and issues. *Int. J. Precis. Eng. Manuf. Green Technol.* **2017**, *4*, 113–125. [CrossRef]
4. Fitch, E.C. *Proactive Maintenance for Mechanical Systems*; Elsevier: Amsterdam, The Netherlands, 2013.
5. Mehmanparast, A.; Taylor, J.; Brennan, F.; Tavares, I. Experimental investigation of mechanical and fracture properties of offshore wind monopile weldments: SLIC interlaboratory test results. *Fatigue Fract. Eng. Mater. Struct.* **2018**, *41*, 2485–2501. [CrossRef]
6. Jadav, H.H.; Badheka, V.; Sharma, D.K.; Upadhyay, G. A review on effect of friction stir processing on the welded joints. *Mater. Today Proc.* **2020**. [CrossRef]
7. Kumar, A.; Sundarrajan, S. Optimization of pulsed TIG welding process parameters on mechanical properties of AA 5456 Aluminium alloy weldments. *Mater. Des.* **2009**, *30*, 1288–1297. [CrossRef]
8. Senthil Kumar, T.; Balasubramanian, V.; Sanavullah, M.Y. Influences of pulsed current tungsten inert gas welding parameters on the tensile properties of AA 6061 aluminium alloy. *Mater. Des.* **2007**, *28*, 2080–2092. [CrossRef]
9. Balasubramanian, V.; Ravisankar, V.; Reddy, G.M. Effect of pulsed current welding on mechanical properties of high strength aluminium alloy. *Int. J. Adv. Manuf. Technol.* **2008**, *36*, 254–262. [CrossRef]
10. Karunakaran, N.; Balasubramanian, V. Effect of pulsed current on temperature distribution, weld bead profiles and characteristics of gas tungsten arc welded aluminium alloy joints. *Trans. Nonferrous Met. Soc. China* **2011**, *21*, 278–286. [CrossRef]
11. Shanavas, S.; Dhas, J.E.R.; Murugan, N. Weldability of marine grade AA 5052 aluminium alloy by underwater friction stir welding. *Int. J. Adv. Manuf. Technol.* **2018**, *95*, 4535–4546. [CrossRef]
12. Sun, Q.J.; Xie, X. Microstructure and mechanical properties of TA15 alloy after thermo-mechanical processing. *Mater. Sci. Eng: A* **2018**, *724*, 493–501. [CrossRef]
13. Park, S.-H.; Lee, H.-K.; Kim, J.-Y.; Chung, H.-T.; Park, Y.-W.; Kang, C.-Y. Effect of welding condition on microstructures of weld metal and mechanical properties in Plasma-MIG hybrid welding for Al 5083 alloy. *J. Weld. Join.* **2015**, *33*, 61–71. [CrossRef]
14. Fuller, C.B.; Mahoney, M.W. The effect of friction stir processing on 5083-H321/5356 Al arc welds: Microstructural and mechanical analysis. *Metall. Mater. Trans. A* **2006**, *37*, 3605–3615. [CrossRef]
15. AzimiRoeen, G.; Kashani-Bozorg, S.F.; Nosko, M.; Lotfian, S. Mechanical and Microstructural Characterization of Hybrid Aluminium Nanocomposites Synthesised from an Al–Fe3O4 System by Friction Stir Processing. *Met. Mater. Int.* **2020**, *26*, 1441–1453. [CrossRef]
16. Habibi, N.; Gangaraj, S.M.; Farrahi, G.H.; Majzoobi, G.H.; Mahmoudi, A.H.; Daghigh, M.; Yari, A.; Moridi, A. The effect of shot peening on fatigue life of welded tubular joint in offshore structure. *Mater. Des.* **2012**, *36*, 250–257. [CrossRef]
17. Sidhom, N.; Laamouri, A.; Fathallah, R.; Braham, C.; Lieurade, H.P. Fatigue strength improvement of 5083 H11 Al-alloy T-welded joints by shot peening: Experimental characterisation and predictive approach. *Int. J. Fatigue* **2005**, *27*, 729–745. [CrossRef]
18. Reddy, G.M.; Gokhale, A.A.; Rao, K.P. Optimisation of pulse frequency in pulsed current gas tungsten arc welding of aluminium–lithium alloy sheets. *Mater. Sci. Technol.* **1998**, *14*, 61–66. [CrossRef]
19. Rao, S.R.K.; Reddy, G.M.; Kamaraj, M.; Rao, K.P. Grain refinement through arc manipulation techniques in Al–Cu alloy GTA welds. *Mater. Sci. Eng. A* **2005**, *404*, 227–234. [CrossRef]
20. Heidarzadeh, A.; Mironov, S.; Kaibyshev, R.; Çam, G.; Simar, A.; Gerlich, A.; Khodabakhshi, F.; Mostafaei, A.; Field, D.; Robson, J. Friction stir welding/processing of metals and alloys: A comprehensive review on microstructural evolution. *Prog. Mater. Sci.* **2020**, 100752. [CrossRef]
21. Mishra, R.S.; Ma, Z.Y. Friction stir welding and processing. *Mater. Sci. Eng. R Rep.* **2005**, *50*, 1–78. [CrossRef]
22. Mabuwa, S.; Msomi, V. Effect of Friction Stir Processing on Gas Tungsten Arc-Welded and Friction Stir-Welded 5083-H111 Aluminium Alloy Joints. *Adv. Mater. Sci. Eng.* **2019**, *2019*, 3510236. [CrossRef]
23. Ikumapayi, O.M.; Akinlabi, E.T. Recent Advances In Keyhole Defects Repairs Via Refilling Friction Stir Spot Welding. *Mater. Today Proc.* **2019**, *18*, 2201–2208. [CrossRef]
24. da Silva, J.; Costa, J.M.; Loureiro, A.; Ferreira, J.M. Fatigue behaviour of AA6082-T6 MIG welded butt joints improved by friction stir processing. *Mater. Des.* **2013**, *51*, 315–322. [CrossRef]
25. Costa, J.D.M.; Jesus, J.S.; Loureiro, A.; Ferreira, J.A.M.; Borrego, L.P. Fatigue life improvement of mig welded aluminium T-joints by friction stir processing. *Int. J. Fatigue* **2014**, *61*, 244–254. [CrossRef]
26. Mandal, P. Surface modification of Aluminium alloy (7xxx series) by multipass friction stir processing. *Glob. J. Eng. Technol. Adv.* **2021**, *6*, 008–017. [CrossRef]
27. Mehdi, H.; Mishra, R. Investigation of mechanical properties and heat transfer of welded joint of AA6061 and AA7075 using TIG+ FSP welding approach. *J. Adv. Join. Process.* **2020**, *1*, 100003. [CrossRef]

28. Meng, X.; Huang, Y.; Cao, J.; Shen, J.; dos Santos, J.F. Recent progress on control strategies for inherent issues in friction stir welding. *Prog. Mater. Sci.* **2021**, *115*, 100706. [CrossRef]
29. ASTM E8 / E8M-21. Standard Test Methods for Tension Testing of Metallic Materials. 2021. [CrossRef]
30. David, S.; Babu, S.; Vitek, J. Welding: Solidification and microstructure. *Jom* **2003**, *55*, 14–20. [CrossRef]
31. AzimiRoeen, G.; Kashani-Bozorg, S.F.; Nosko, M.; Orovcik, L. EBSD investigation of Al/(Al13Fe4+ Al2O3) nanocomposites fabricated by mechanical milling and friction stir processing. *J. Microsc.* **2018**, *270*, 3–16. [CrossRef]
32. Azimi-Roeen, G.; Kashani-Bozorg, S.F.; Nosko, M.; Orovcik, L.; Lotfian, S. Effect of multi-pass friction stir processing on textural evolution and grain boundary structure of Al–Fe3O4 system. *J. Mater. Res. Technol.* **2020**, *9*, 1070–1086. [CrossRef]
33. McNelley, T.R.; Swaminathan, S.; Su, J.Q. Recrystallisation mechanisms during friction stir welding/processing of aluminium alloys. *Scr. Mater.* **2008**, *58*, 349–354. [CrossRef]
34. Huang, K.; Logé, R.E. A review of dynamic recrystallisation phenomena in metallic materials. *Mater. Des.* **2016**, *111*, 548–574. [CrossRef]
35. Heidarzadeh, A.; Saeid, T.; Klemm, V.; Chabok, A.; Pei, Y. Effect of stacking fault energy on the restoration mechanisms and mechanical properties of friction stir welded copper alloys. *Mater. Des.* **2019**, *162*, 185–197. [CrossRef]
36. Quek, S.S.; Chooi, Z.H.; Wu, Z.; Zhang, Y.W.; Srolovitz, D.J. The inverse hall–petch relation in nanocrystalline metals: A discrete dislocation dynamics analysis. *J. Mech. Phys. Solids* **2016**, *88*, 252–266. [CrossRef]